Environmental Earth Sciences (2018) 77:17
https://doi.org/10.1007/s12665-017-7201-9

ORIGINAL ARTICLE

On the technical properties of the Carovigno stone from Apulia (Italy): physical characterization and decay effects by means of experimental ageing tests

Giovanna Fioretti[1] · Paolo Mazzoleni[2] · Pasquale Acquafredda[1,3] · Gioacchino Francesco Andriani[1]

Received: 28 March 2017 / Accepted: 29 December 2017 / Published online: 11 January 2018

Abstract
Apulia (southern Italy) is typified by widespread outcrops of rocks exploited in the last centuries in historical architectures and religious constructions, as building and decorative stone. Today, as in the past, these stones represent an important source for region economy and prestige, due to their uses for modern works, restoration of local medieval churches and also exporting abroad. Among these, a noteworthy and still poorly known material is the Carovigno stone. In this paper, firstly an overall view on the, mineralogical and petrophysical features of the stone was reached through a multianalytical approach based on several investigation procedures and techniques, including ultrasonic test, X-ray diffractometry, scanning electron microscopy, optical microscopy, mercury intrusion porosimetry. In order to simulate decay phenomena, the Carovigno stone samples were processed to three different ageing tests: cycles of thermal treatments at different high temperatures, cycles of heating–cooling and cycles of exposure to decahydrate sodium sulphate and sodium chloride saline solutions. During and after each ageing processes, mineralogical transformations and petrophysical changes were evaluated. Results suggested that the Carovigno stone is a fine-grained calcarenite, pure or nearly pure, characterized by high porosity and, consequently, very notable thermal stress resistance. Conversely, the type and amount of porosity causes stone predisposition to salt crystallization decay.

Keywords Carovigno stone · Stone characterization · Ageing test · Decay · Apulia

Introduction

The Carovigno stone

In the Apulia region (southern Italy), Cretaceous shallow-water limestones are widespread and form a continuous and flat layer, some thousand metres thick (Spalluto and Caffau 2010). By virtue of geological features and stone suitability to be exploited, in this geographic area, mining activities are enhanced since time and uses of stone in the region have a centuries-old tradition. Indeed, local inhabitants employed their stone resources to build and adorn churches, castles and other religious and civil buildings. In the region, decorative stone industry is today extremely profitable, thanks to high productivity and performance of several quarries; therefore, Apulia could be considered one of the most developed mining area, not only in Italy but also in an international framework. The stone industry counts more than 1500 companies which produce a turnover of over 29 million euro every year. Moreover, scientific

✉ Giovanna Fioretti
giovafioretti@gmail.com

Paolo Mazzoleni
pmazzol@unict.it

Pasquale Acquafredda
pasquale.acquafredda@uniba.it

Gioacchino Francesco Andriani
gioacchinofrancesco.andriani@uniba.it

[1] Department of Earth and Geoenvironmental Sciences, University of Bari Aldo Moro, Bari, Italy

[2] Department of Biological, Geological and Environmental Sciences, University of Catania, Catania, Italy

[3] Interdepartmental Centre of Laboratory of Research for Diagnostic of Cultural Heritage, University of Bari Aldo Moro, Bari, Italy

research is focusing on these building and ornamental materials, both in finding and opening of new quarries and in improvement of stone behaviour, when exposed to environmental damaging agents. Concurrently, in addition to the diffusion of hard and medium-hard limestones from the famous extraction basins of Apricena and Trani, very close to marble for appearance, also medium-soft and soft calcarenites, such as the Leccese stone (Calia et al. 2014; Cherubini et al. 2007), the Ostuni stone (Tucci and Morbidelli 2004; Tucci et al. 2007) and "Calcareous Tufa", belonging to the Calcarenite di Gravina Fm. (Andriani and Walsh 2010), are noteworthy. Thanks to their easy workability, they have been used in masonry, as construction material, or for embellishment purpose in fanlight, capitals, sculptures and other decorative elements of architectonical facades, in fountains, monuments. A less known material is the Carovigno stone, which is a fine, white and medium-soft calcarenite, mined in a quarry located in Carovigno, near Brindisi (Fig. 1a).

In virtue of its aesthetical appeal and its local widespread availability, the Carovigno stone was locally employed as building material especially in old civil and religious architectures. Nevertheless, its use is probably underestimated because of its similarity with the more famous Ostuni stone, extracted only few kilometres from Carovigno. However, the stone has been recognized in some historic monuments and religious buildings of the region, both as construction material and as replacement material during restorations of last centuries. Very notable examples are the Dentice di Frasso castle (Fig. 1b), belonging to Normans period (11th century), the St. Anne church (Fig. 1c), built in the 17th century, both in Carovigno, and the Maddalena church in Mola di Bari, risen in the 17th century.

The source area of the Carovigno stone is located in Contrada Centopezze, on the Adriatic side of the Murge plateau, in the Southeast sector of the Apulian region, about 25 km North–West from Brindisi, in the Carovigno district. The Murge plateau, an emergent part of the Apulian Foreland, is characterized by 3-km-thick Cretaceous succession, consisting of platform limestones and dolostones, which are overlain by transgressive discontinuous and thin calcarenites, dated to Plio-Pleistocene (Ricchetti et al. 1988). The Carovigno stone includes fine to medium-grained homogeneous and closely packed calcarenites belonging to an informal lithostratigraphic unit known as "Calcare di Caranna" (late Campanian?–Maastrichtian); the last is a slope-basin bioclastic deposit that comprises fine to coarse-grained prograding calcarenites cropping out in the SE Murge plateau (Luperto Sinni and Borgomano 1989; Luperto Sinni 1996).

Accelerated ageing test and stone decay

Generally, the stone decay is strictly related to void volume and structure. Pore network in the material represents the main way for the entry and movement of water, which is considered the most dangerous vehicle of pollutants. This aspect is particularly troubling when stones are employed as building and decorative materials, because it causes modification and decay of valuable Cultural Heritage. In calcareous rocks, porosity increasing is connected mainly to the action of water inside voids and fractures of stone and to the thermal behaviour. The actions of water principally consist in freeze–thaw phenomena and crystallization of salts dissolved in water (Lazzarini and Laurenzi Tabasso 1986). Thermal effects are connected to the strong thermal expansion anisotropy of calcite crystals, which produce

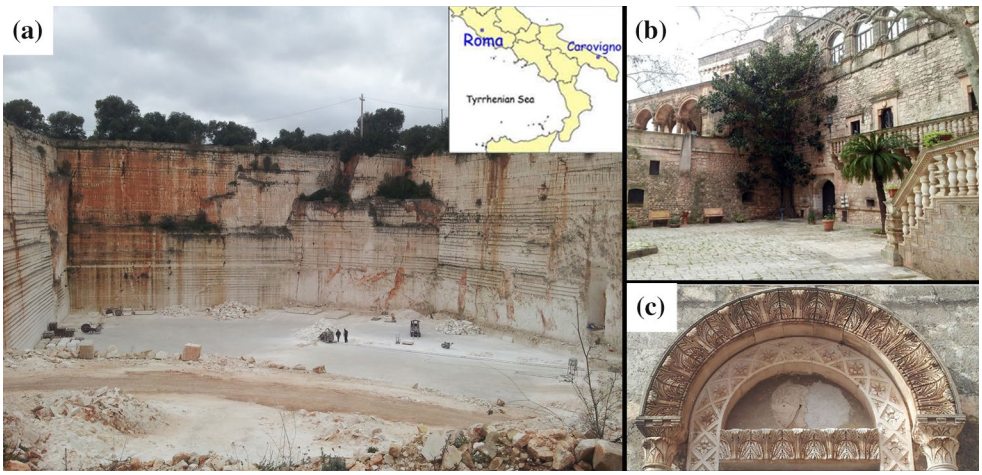

Fig. 1 The Carovigno stone quarry, located in Contrada Centopezze, near Carovigno (**a**); Dentice di Frasso Castle (**b**), Carovigno (Apulia, southern Italy): the use of the Carovigno stone is certified both in the walls, as building material, and in the balustrades and other decorative elements, as ornamental stone; St. Anna Church (**c**), Carovigno, focus on portal: image shows different decorative motifs carved in the Carovigno stone

simultaneously detachments and stresses on grain edges (Siegesmund et al. 2000). Accelerated ageing tests allow engendering artificial decay on materials. Several authors suggest methods for implementation of ageing tests. In strong thermal treatments, also to simulate fire action, and thermal shocks (heating–cooling), samples could be exposed to very high temperatures and to thermal changes from high to low temperatures and vice versa, respectively (Allison and Bristow 1999; Mutluturk et al. 2004; Yavuz et al. 2006, 2010; Sippel et al. 2007; Cantisani et al. 2009; Franzoni et al. 2013; Andriani and Germinario 2014; Vázquez et al. 2016). Referring to salt crystallization, researchers follow to UNI EN 12370:2001, which recommends cycles of immersion in $Na_2SO_4 \cdot 10H_2O$ solution and later drying of samples, to allow salt precipitation in pores (Rothert et al. 2007; Molina et al. 2011; Barbera et al. 2012; Anania et al. 2012). Nevertheless, the test can be executed using other saline compounds such as sodium, magnesium, calcium and potassium sulphates, sodium and calcium chlorides (Cardell et al. 2003; Ruiz-Agudo et al. 2007; El-Gohary 2011) and even sea water (Andriani and Walsh 2007).

Experimental method

The method was based on a multianalytical approach and consisted of three step: the characterization of the Carovigno stone, its artificial ageing by means of different procedures and characterization of the decayed stone. Firstly, samples of studied material were collected from the quarry and shaped in 5 cm cubes. Chromatic features were evaluated in a CIELab colour space, by a Konica Minolta CM2600-d portable spectrophotometer, using a D65 illuminant, a 2° observer and an 8 mm target mask. On each sample, before and after ageing treatments, 9 measures of colour were recorded. X-ray diffraction analysis was performed using a Philips 1730/10 instrument; Ni-filtered CuKα radiation was used and the spectra were elaborated with the Panalytical High Score software. Petrographic study on thin section was carried out by a Zeiss Axioskop 40 optical microscope equipped with a 5.2 Mpx CCD. Further observations were obtained through scanning electron microscopy LEO, EVO50XVP model coupled with an X-max (80 mm^2) Silicon drift Oxford equipped with a Super Atmosphere Thin Window. Operating conditions of SEM were: 15 kV accelerating potential, 500 pA probe current and 8.5 mm working distance. Before SEM investigations, samples were fixed on an aluminium stub with colloidal graphite and then sputtered with a 30-nm-thick carbon film using an Edwards Auto 306 thermal evaporator. In terms of physical properties, water absorption coefficient by capillarity was defined following EN 1925: 2000: 50 mm cubic samples of material were placed in a container filled of water up to 3 mm and weighted after established time of 1, 3, 5, 10, 30, 60 min and 2, 3, 8, 24, 48, 72 h.

Porosimetric data were obtained by mercury intrusion porosimetry following ASTM D 4404-84 (1999) and operating by a Micromeritics AutoPore IV 9500 porosimeter, both in low (3.44–345 kPa) and high pressure (0.1–228 MPa), detecting pore diameters between 410 and 0.005 µm. Ultrasound propagation velocity in rock samples was performed by a Pundit instrument (CNS Electronics Ltd), according to EN 14579:2004 and operating with the direct method, placing the 54 kHz transducers on the opposite faces of the samples. The average between three measures along the three-cube axis was considered.

The second stage involved different ageing tests. The exposure at high temperatures was carried out on samples from 200 to 500 °C in 8 cycles of 24 h for 192 h. For the overall test, 12 samples were involved, specifically 3 samples for each programme. At the end of every cycle, samples were removed from muffle furnace and placed in a dryer to cool up to room temperature in dry environment. Regarding thermal shock, the test was performed heating 6 samples at 105 °C for 8 h followed by immediate transfer in water at 20 °C for 16 h. Sequence was repeated for 80 cycles. Finally, in the salt crystallization ageing test, 6 samples were immersed in 14% $Na_2SO_4 \cdot 10H_2O$ solution for 8 h and after dried in a muffle furnace at 105 °C for 16 h. Test ends after 12 cycles. The same procedure was adopted for exposure of other 6 samples to NaCl solution. After every cycle, the mass loss was measured with analytical balance.

In the last step, changes in the materials, in terms of chromatic and visual appearances, mass loss, mineralogical compositions, ultrasound propagation velocity, capillarity index and porosity, were recorded.

Results

Fresh stone characterization

Mineralogical investigation carried out through XRPD analysis revealed that the studied stone was composed almost exclusively by calcite.

Thin-section analysis carried out with optical polarized microscope allowed us to describe the general petrographic features of these carbonate rocks. They are mainly made up of coated grains ranging from 0.1 to 0.4 mm in diameter: they are irregularly shaped peloids that often merge into the surrounding carbonate mud. Bioclastic fragments with a regular elongated morphology have been recognized. They are prismatic mollusc fragments. Rare and poorly preserved foraminifers occur. The no-carbonatic particles are rare brown-reddish iron hydroxides. Rare is the presence of opaque minerals. Cementation is regularly distributed in

the rock, and it is microsparitic in size. Primary porosity is typically made up of interparticle irregular voids. Regular sub-millimetre fractures with a linear development have been recognized: they are cicatrized by spatic calcite. Spatic calcite also fills the voids of fossils. According to the classification of Dunham (1962), the rock could be classified as packstone (Fig. 2a).

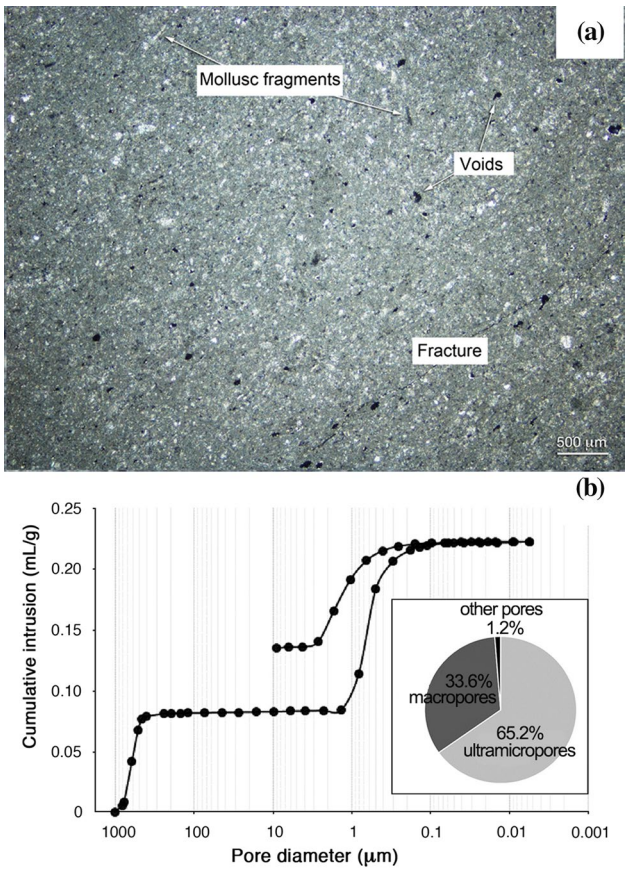

Fig. 2 Microphotograph (**a**) of the Carovigno stone (N+), showing typical porosity and micrite and microfossils content; porosimetric curve (**b**) obtained from MIP analysis on fresh samples; in the box the pore size distribution according to Brewer (1964) classification

As regards the physical properties, an average dry density of 1.9 g/cm^3 was calculated and porosity was measured by mercury intrusion porosimetry (MIP). The latter revealed that samples were characterized by an open porosity of 37%; the cumulative volume vs. pore diameter graph (Fig. 2b) indicated a bimodal pore distribution, due to the contribution of macropores (pore diameter > 75 µm) and of ultramicropores (0.1 µm < pore diameter < 5 µm), following the Brewer (1964) classification. A small percentage of pores (1.2%) were mesopores, micropores and cryptopores therefore, because of their insignificance, they were grouped in a single category, named "other pores".

Moreover, the mercury intrusion–extrusion curve shape suggested the presence of predominant bottleneck pores. Water absorption by capillarity test revealed that samples absorbed very quickly and similarly for the three axes of cubic samples. These data confirm the stone isotropy and the absence of discontinuities, previously observed by visual examination.

Artificially decayed stone characterization

Samples of Carovigno stone were aged by 8 cycles, each lasting for 24 h, of thermal treatment at high temperatures, from 200 to 500 °C (Fig. 3a). After treatments, samples maintained their shape and mass values (Table 1). Visible effects of induced decay did not occur, except for a very slight chromatic change ($\Delta E_{200\ °C} = 1.53$; $\Delta E_{300\ °C} = 3.61$; $\Delta E_{400\ °C} = 3.7$; $\Delta E_{500\ °C} = 3.74$). As expected, high temperature did not produce the dissociation of calcite nor other

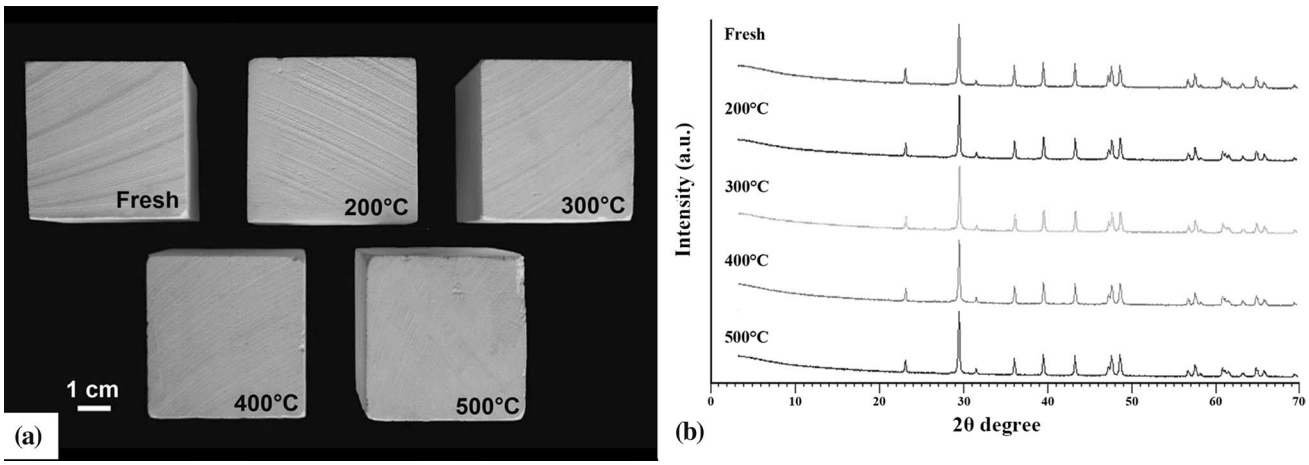

Fig. 3 Photographs of the fresh sample and after increasing temperature treatments (**a**): with temperature increasing no significant changes are revealed in the samples; XRD spectra (**b**) of untreated sample powder and sample powder after thermal treatments: XRD interpretation revealed that spectrum peaks were distinctive of calcite and plots show a perfect fit of mineralogical patterns

Table 1 Mass variation (%), ultrasonic velocity variation (%) and its standard deviation (%) measured on samples before treatments and after each cycle at different temperatures (200–300–400–500 °C)

		200 °C	300 °C	400 °C	500 °C
t_0	Δm	–	–	–	–
	ΔUPV	–	–	–	–
	ΔUPV St.Dev.	–	–	–	–
24 h	Δm	0.01	0.03	0.05	0.09
	ΔUPV	7.36	3.79	29.81	43.88
	ΔUPV St.Dev.	2.75	1.23	0.43	0.10
48 h	Δm	0.01	0.03	0.05	0.10
	ΔUPV	8.17	− 8.45	31.20	43.58
	ΔUPV St.Dev.	0.40	1.06	0.43	0.66
72 h	Δm	0.02	0.03	0.06	0.11
	ΔUPV	8.17	− 2.92	33.98	46.87
	ΔUPV St.Dev.	2.16	6.95	0.58	0.33
96 h	Δm	0.01	0.03	0.06	0.12
	ΔUPV	6.54	− 4.96	35.38	46.27
	ΔUPV St.Dev.	1.43	0.73	0.22	0.48
120 h	Δm	0.02	0.03	0.07	0.12
	ΔUPV	3.81	− 6.71	36.49	49.55
	ΔUPV St.Dev.	2.45	2.03	0.36	0.04
144 h	Δm	0.01	0.04	0.06	0.14
	ΔUPV	10.63	− 4.08	31.75	46.27
	ΔUPV St.Dev.	3.14	2.50	1.13	0.04
168 h	Δm	0.02	0.04	0.07	0.14
	ΔUPV	7.08	− 6.41	35.93	47.16
	ΔUPV St.Dev.	2.24	1.64	1.94	0.27
192 h	Δm	0.02	0.04	0.07	0.15
	ΔUPV	8.99	− 2.33	34.26	47.46
	ΔUPV St.Dev.	0.63	0.38	0.12	0.46

mineralogical transformation; XRPD analysis revealed a perfect fit of untreated and heated sample X-ray spectra (Fig. 3b).

SEM investigation revealed that sample surface morphology was quite comparable, in terms of shape and size of calcite crystals and rock fabric, even after higher temperature treatments (Fig. 4).

Results about ultrasonic test are reported in Table 1 and in the graph in Fig. 5a. In samples before treatment, the mean value of ultrasonic velocity was 3.5 km/s; after 200 °C treatment, ultrasonic velocity slightly decreased (7.4%), whereas in samples after 300 °C treatment, ultrasonic acceleration (3.8%) suggested density increase. Instead, in samples subjected to treatments at 400 and 500 °C, the velocity values were, respectively, 29.8 and 43.9% lower than that measured in fresh sample. In addition, after the first cycle (24 h), ultrasonic velocity lowered proportionally to the treatment temperatures and after stabilized.

The capillarity test was performed after 8 cycles at different temperatures. Absorption profiles showed the same trend and slope in the initial portion of curves (Fig. 5b); generally, in the first 5 min of the test, samples rapidly absorbed water. After absorption, curve continued almost asymptotically, up to the end. Samples treated to 200 °C and fresh samples were characterized by the same absorption index, which was slightly lower than absorption in samples treated to 300 and 400 °C, whereas absorption of 500 °C treated samples was higher than the others.

Mercury intrusion porosimetry results (Table 2) indicated that in samples after 200 °C ageing, porosity was slightly higher (41%) than that measured in fresh samples (37%). In the 300 °C samples, porosity decreased (22%) and in the 400 and 500 °C samples, porosity values were, respectively, 33 and 45%.

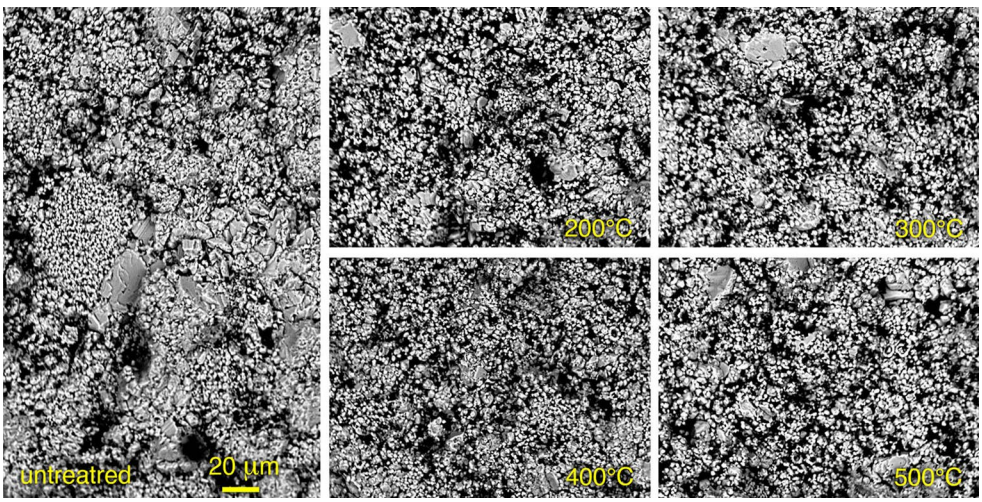

Fig. 4 BSE–SEM images of fresh and high temperatures up to 500 °C treated samples (Operating conditions of SEM: 15 kV accelerating potential, 500 pA probe current and 8.5 mm working distance)

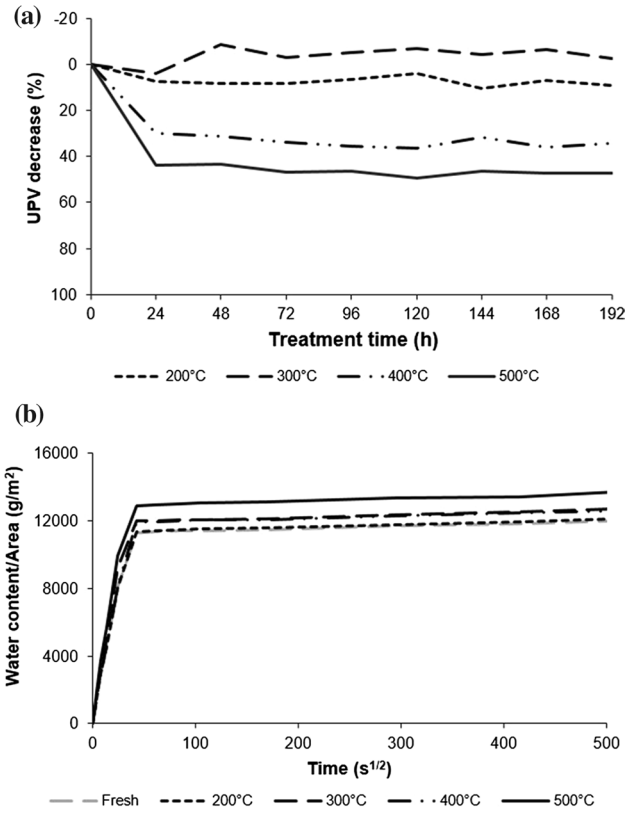

Fig. 5 Ultrasonic velocity (UPV) variation during thermal treatment, for each temperature, measured every 24 h (**a**); Water content/area vs. time relationship in fresh sample and in samples after thermal treatments (**b**)

Table 2 Open porosity of fresh and thermally treated samples, measured by mercury intrusion porosimetry (MIP)

Treatment temperature (°C)	Open porosity (%) by MIP
Fresh	37.5
200	41.3
300	21.6
400	33.4
500	44.8

Graphs reported in Fig. 6 displayed that thermal treatments did not modify as much size distributional of ultramicropores (0.1–5 µm), but rather of 100–1000 µm macropores. In fresh sample, the pore size was about 400–800 µm; after 200 °C treatment, 200–400 µm pores originated and, in 300 °C sample, they disappeared; after 400 °C treatment, 600–800 µm pores remained and 200–400 and 100–200 µm pores appeared; in 500 °C sample, 400–800 µm pore number increased.

The second ageing test was composed of 80 cycles of heating–cooling to simulate thermal shock, which involved a set of six cubic samples of Carovigno stone (Table 3). At the end of the treatment, no clear alteration was observed, in terms of shape, volume and appearance; mass loss lower that 1% and a very light change colour ($\Delta E = 4.41$) were recorded. Every 20 heating–cooling cycles, ultrasonic test was performed. The ultrasonic velocity, which initially was 3.6 km/s (mean value), strongly decreased by about 15.8% after 20 cycles and more gradually in following cycles up to 22.83% after the last cycle.

In the third and last ageing treatment, two groups of six samples were aged using two different salts in solutions, $Na_2SO_4 \cdot 10H_2O$ and NaCl. After the first two cycles in sulphate solution, samples presented a considerable susceptibility to salt damaging action; a progressive decay interested samples, which showed severe material loss from cube corners and alteration of surface appearance (Fig. 7).

For this reason, test was interrupted after 12 cycles. Chromatic changes at the end of test were very low ($\Delta E = 1.57$). In samples after salt crystallization test in sodium chloride solution, the salt growth produced more moderate effects than the previous case, consisting only in formation of surface microholes, without substantial material losses. Also in this case, surface colour change was irrelevant ($\Delta E = 1.07$). After ageing by sodium sulphate solution, the variation of the sample masses (Table 4) was described by a fluctuated trend (Fig. 8a) due to the contrasting effect of the crystallization of mass gain caused by the salt crystallization into the pore and the mass loss of the stone. Ultrasonic test was even carried out on samples after salt crystallization test (Fig. 8b). Velocity value, which was 3.47 km/s before treatment, collapsed of 28.2% after the second cycle and gradually during the treatment up to 54.63% at the end of the ageing. The ultrasonic velocity change was comparable for each samples of set, and the very low standard deviation confirmed the high homogeneity and isotropy of the Carovigno stone.

After treatment in sodium chloride solution, a quick increase in mass values occurred, due to salt precipitation in natural voids of the rock (Fig. 8c). After the next cycles, mass value rise varied between 10 and 13% compared to the initial values (Table 5). In addition, ultrasound velocity decreased (Fig. 8d); however, the behaviour of samples was different from samples aged in sodium sulphate solution. In fact, values reduced sharply by 22.5% after the first two treatment cycles and subjected to a more gradual and fluctuating reduction in subsequent cycles up to reach 33% after the 24th cycle.

Discussion

The mineralogical investigation carried out on the Carovigno stone highlighted that this limestone is composed almost exclusively of calcite crystals. Texture and absence of discontinuities in the material is responsible of homogeneity and isotropy of physical properties, as ultrasound velocity

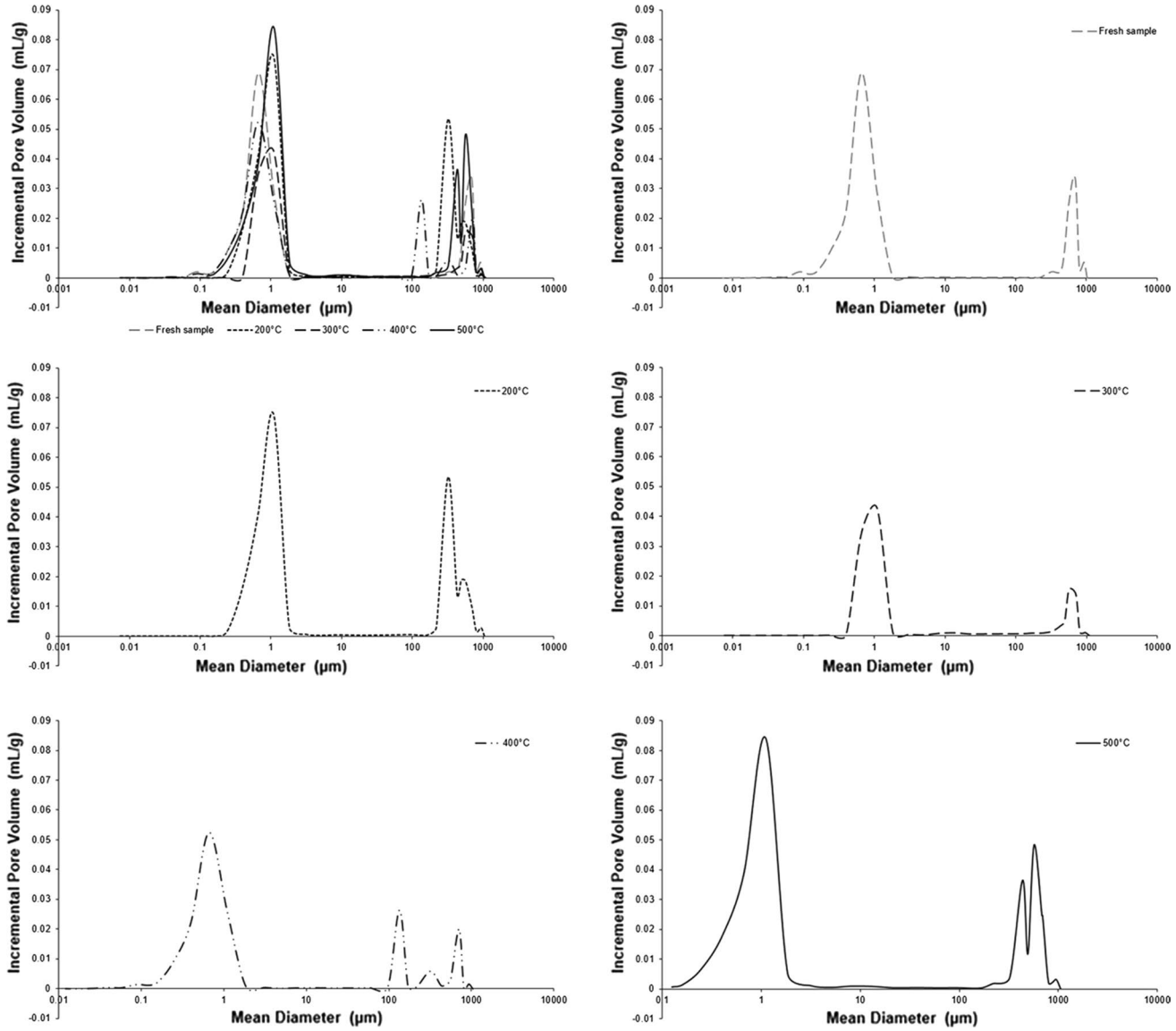

Fig. 6 Incremental pore volume vs. mean diameter in fresh sample and in samples after thermal treatments (in the upper left) and extracts from the previous graph, concerning the incremental pore volume for each thermal treatment (in the other graphs)

Table 3 The ultrasonic velocity variation and its standard deviation measured on samples, before and after 20, 40, 60 and 80 cycles of thermal shock treatment, are reported

t_0		20 cy		40 cy		60 cy		80 cy	
ΔUPV	ΔUPV St.Dev.	ΔUPV	ΔUPV St.Dev.	ΔUPV	ΔUPV St.Dev.	ΔUPV	ΔUPV St.Dev.	ΔUPV	ΔUPV St.Dev.
–	–	15.75	2.82	19.41	3.50	23.29	2.97	22.83	3.27

and capillarity water absorption that are comparable along three orthogonal axes. The Carovigno stone is highly porous and characterized by bimodal distribution of open voids, corresponding to the macropores (> 75 μm) and ultramicropores (0.1–5 μm) groups. This porosity type influences the stone behaviour after stress induced by artificial decay treatments.

As a result of ageing tests, materials revealed high durability to thermal effects, both in terms of resistance to high temperature and in terms of thermal shock. The macroscopic

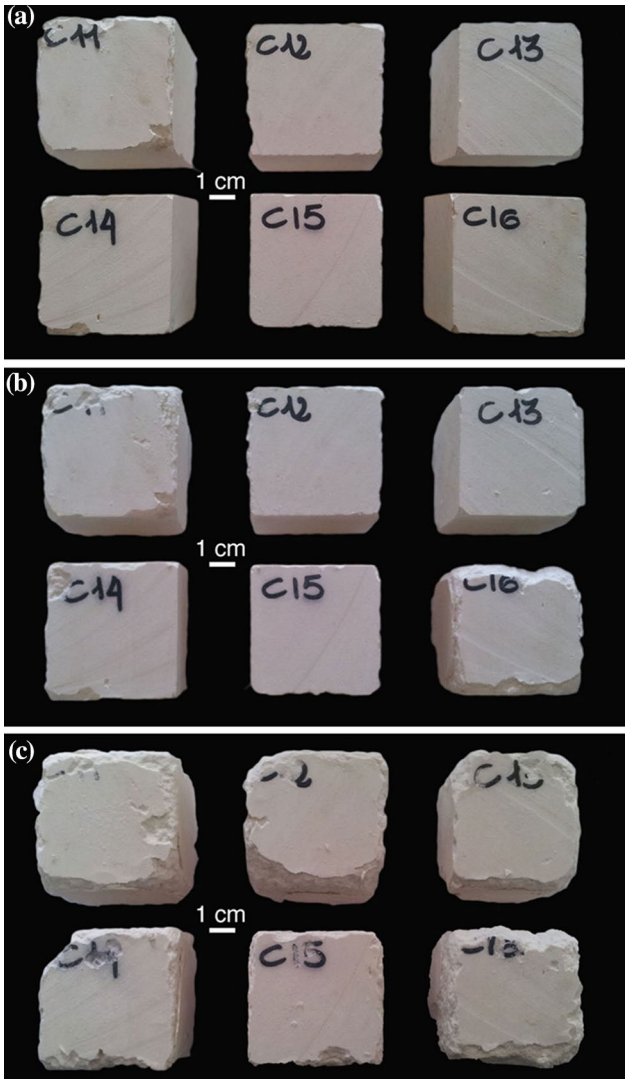

Fig. 7 Macroscopic appearance of samples treated in sodium sulphate solution after 4 (**a**), 8 (**b**) and 12 (**c**) cycles. Samples showed a progressive decay and material loss due to salt growth action

Table 4 Mass variation (%), standard deviation of mass variation (%), ultrasonic velocity variation (%) and its standard deviation are reported for samples before treatments and after 2, 4, 6, 8, 10 and 12 cycles of treatment in sodium sulphate solution

	Δm	Δm St.Dev.	ΔUPV	ΔUPV st.dev.
t_0	–	–	–	–
2 cy	− 3.17	0.24	28.20	1.72
4 cy	− 5.65	0.26	35.44	1.37
6 cy	− 1.82	0.81	35.64	6.17
8 cy	− 2.99	3.1	44.78	2.68
10 cy	− 5.31	4.35	51.76	0.97
12 cy	− 1.53	3.31	54.63	1.34

appearance suffered no volume and shape modifications. Moreover, the colour did not change except for samples after 400 and 500 °C treatments, which showed a barely perceptible chromatic alteration. Moreover, the mineralogical composition did not suffer modification as well as porosity distribution and capillarity index. Ultrasonic test was proved to be very useful to understand the behaviour of thermally treated samples. Reduction in ultrasound velocity values is generally connected to the increasing of the porosity and the consequent decrease of density, due to the microcracking. Only the ultrasonic velocity values in samples after high temperature treatments (400 and 500 °C) strongly decreased.

The high resistance to thermal stresses is explainable considering the large void volume that, on the one hand, reduces heat transfer and, on the other, ensures available space for the expansion of calcite crystals, without sensible cracking production or increasing in the material. Moreover, all the results mainly from ultrasonic test and mercury intrusion microporosimetry are strongly in agreement and clearly suggest that two opposite processes coexist in this carbonate rock during thermal treatment. On the one hand, calcite crystal expansions, due to thermal contribution, arise and a residual expansion remains, as consequence of repeated heating–cooling cycles; in this way, partial closing of the voids happens and therefore a density increasing. On the other hand, calcite has a thermal anisotropic behaviour; hence, crystals expand along c axis and decrease in size along a and b axes; it produces detached between near crystals and simultaneously mechanical stresses which cause microcracking. In this sense, MIP and ultrasonic test results indicate that, after 200 °C treatment, the two contributions could be considered comparable, even though a little reduction in ultrasound velocity was recorded. In samples after 300 °C ageing, void closing prevails on microcracking growth: this is due to the increasing in size of the little calcite crystals which, growing in one direction, occupy the volume of a little void, when present; conversely, although the void space was reduced after expansion of calcite crystals, in 400 and 500 °C samples, fractures extend and new cracks develop, reason why porosity increases and ultrasonic velocity reduces. Pore-size distribution, obtained by MIP, reveals that thermal treatments mainly involve macropores (100–1000 μm) and ultramicropores (0.1–5 μm). After 200 °C treatment, new pores (200–400 μm diameter) appeared and after 300 °C treatment disappeared as a consequence of their closure. After 400 °C, they re-formed and also 100–200 μm appeared because microcracking advances involving calcite single crystals. Finally, in 500 °C samples, larger pores (300–800 μm diameter) replace smaller pores, which are subjected to widening due to the thermal effect.

After thermal shock simulations, samples displayed a remarkable resistance to heat action, since they preserved their macroscopic features, such as colour and shape.

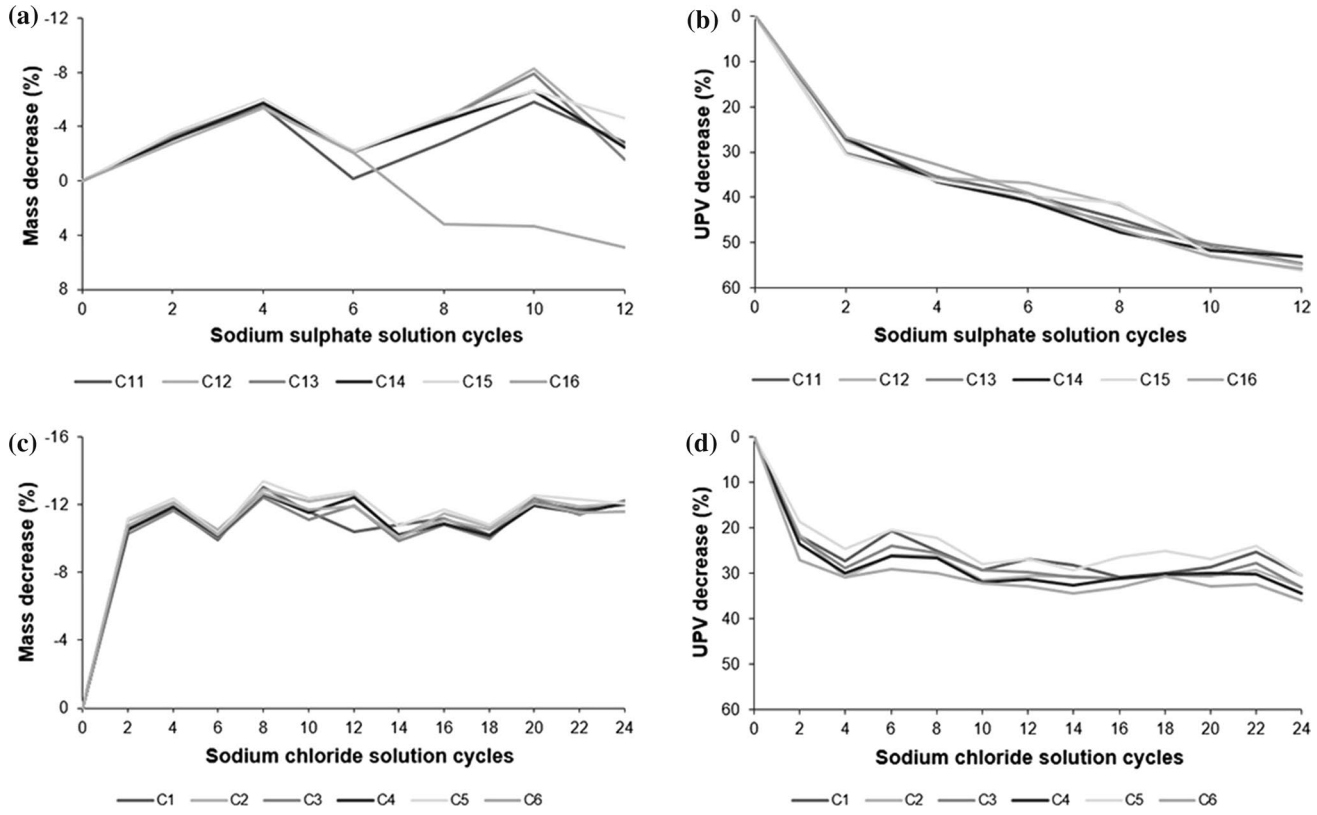

Fig. 8 Mass loss (**a**) and ultrasonic velocity (UPV) reduction (**b**) in samples treated in decahydrate sodium sulphate solution, measured every two cycles; mass loss (**c**) and ultrasonic velocity reduction (**d**) in samples treated in sodium chloride solution, measured every two cycles

Table 5 Mass variation (%), standard deviation of mass variation (%), ultrasonic velocity variation (%) and its standard deviation are reported for samples before treatments and after every 2 cycles up to the end of treatment in sodium chloride solution

	Δm	Δm st.dev.	ΔUPV	ΔUPV st.dev.
t_0	–	–	–	–
2 cy	− 10.73	0.33	22.47	2.79
4 cy	− 11.99	0.27	28.81	2.44
6 cy	− 10.19	0.22	24.44	3.41
8 cy	− 12.85	0.35	26	2.46
10 cy	− 11.76	0.45	30.46	1.7
12 cy	− 12.02	0.85	29.81	2.45
14 cy	− 10.29	0.39	31.01	2.22
16 cy	− 11.19	0.35	30.7	2.21
18 cy	− 10.39	0.33	29.48	2.19
20 cy	− 12.25	0.21	29.96	2.01
22 cy	− 11.74	0.33	28.27	3.16
24 cy	− 12.01	0.23	32.96	2.22

However, reduction in ultrasound velocity values testifies light microcrack intensification and pore broadening, even if visible effects did not occur. In contrast to high temperature treatments, the reduction in ultrasound velocity was more pronounced after the first step of treatment (20 cycles), but continued gradually in next cycles.

Although porosity of the Carovigno stone represents an advantage in terms of its thermal durability, it is dangerous because it allows entry and movement of water and its harmful compounds. Effectively, ageing through salt crystallization test produces marked decay effects, given by considerable material loss from the edges. The observed fluctuation of mass values during both salt crystallization tests could be explained by the occurring of two phases, which are continuously and cyclically repeated. In the first one, salt crystals precipitate in natural voids of material, without causing damage; in the second stage, the growth and the further precipitation of salt nuclei determine mechanical destructive action which leads to the formation of new fractures and, thus, a second porosity generation. As expected, the action of sodium sulphate precipitation was more damaging than that of sodium chloride, principally due to its higher volume expansion. Saline solution penetrated through open pores and circulated inside; nevertheless, the decay, produced after salt growth, interested mainly the more external portion of cubic samples.

Conclusion

The Carovigno stone can be considered a very good stone, certain in virtue of its easy workability, local large availability and pleasant white colour, given by the mineralogical pure composition. Its main strength is the durability in terms of thermal shock and high or extreme temperatures resistance. Porosity, together with the presence of only calcite crystals, on the one hand ensures a low heat propagation in the stone, and on the other hand a "pillow effect" concerning to thermal expansion of calcite crystals. This causes lower spread of microcracking and thus aesthetic appearance and physical performances conservation. Differently, the Carovigno stone is more sensitive to the action of salts in solution quite because of its porosity; nevertheless, in this case, the damage caused by salt growth involves only the surface layers or localized areas, since pores are poorly connected to each other and then saline solution movement is restricted. This could be a good starting point for the future research to test innovative materials for the consolidation and protection of stone from harmful salt crystallization.

Acknowledgements This research was supported by MIUR (Italian Ministry of Education, University and Research) ex MURST 60%. Many thanks to Mr. Marcello Andriani of the Leo Martino company, for providing samples of the Carovigno stone, essential for this experimental research.

References

Allison RJ, Bristow GE (1999) The effects of fire on rock weathering: some further considerations of laboratory experimental simulation. Earth Surf Proc Landf 24:707–713

Anania L, Badalà A, Barone G, Belfiore CM, Calabrò C, La Russa MF, Mazzoleni P, Pezzino A (2012) The stones in monumental masonry buildings of the ''Val di Noto'' area: new data on the relationships between petrographic characters and physical–mechanical properties. Constr Build Mater 33:122–132

Andriani GF, Germinario L (2014) Thermal decay of carbonate dimension stones: fabric, physical and mechanical changes. Environ Earth Sci 72(7):1–17

Andriani GF, Walsh N (2007) The effect of wetting and drying, and marine salt crystallization on calcarenite rocks used as building material in historic monuments. In: Prikryl R, Smith BJ (eds) Building stone decay: from diagnosis to conservation, vol 271. Geological Society London, Special Publications, London, pp 179–188

Andriani GF, Walsh N (2010) Petrophysical and mechanical properties of soft and porous building rocks used in Apulian monuments (south Italy). Geol Soc Lond Spec Publ 333:129–141

ASTM D 4404-84 (1999) Standard test method for determination of pore volume and pore volume distribution of soil and rock by mercury intrusion porosimetry, designation D 4404-84 (Reapproved 1992). Annual Book of ASTM Standards 04.08:588–592

Barbera G, Barone G, Mazzoleni P, Scandurra A (2012) Laboratory measurement of ultrasound velocity during accelerated aging tests: implication for the determination of limestone durability. Constr Build Mater 36:977–983

Brewer R (1964) Fabric and mineral analysis of soils. Wiley, New York

Calia A, Laurenzi Tabasso M, Mecchi AM, Quarta G (2014) The study of stone for conservation purposes: Lecce stone (southern Italy). Geol Soc Lond Spec Publ 391:139–156

Cantisani E, Pecchioni E, Fratini F, Garzonio CA, Malesani P, Molli G (2009) Thermal stress in the Apuan marbles: relationship between microstructure and petrophysical characteristics. Int J Rock Mech Min 46:128–137

Cardell C, Delalieux F, Roumpopoulos K, Moropoulou A, Auger R, Van Grieken R (2003) Salt-induced decay in calcareous stone monuments and buildings in a marine environment in SW France. Constr Build Mater 17:165–179

Cherubini C, Reina A, Bruno D (2007) Le rocce tenere del Salento: proposta di classificazione con l'uso delle caratteristiche tecniche e meccaniche. Geologi e Territorio 2:34–47

Dunham RJ (1962) Classification of carbonate rocks according to depositional texture. Am Assoc Pet Geol 1:108–121

El-Gohary M (2011) Chemical deterioration of Egyptian limestone affected by saline water. Int J Conserv Sci 2(1):17–28

EN 12370 (2001) Metodi di prova per pietre naturali. Determinazione della resistenza alla cristallizzazione dei sali. CNR-ICR, Rome

EN 14579 (2004) Natural stone test methods—determination of sound speed propagation. CEN, Brussels

EN 1925 (2000) Metodi di prova per pietre naturali. Determinazione del coefficiente di assorbimento d'acqua per capillarità. CNR-ICR, Rome

Franzoni E, Sassoni E, Scherer GW, Naiduc S (2013) Artificial weathering of stone by heating. J Cult Herit 14(3):e85–e93

Lazzarini L, Laurenzi Tabasso M (1986) Il restauro della pietra. CEDAM, Padova

Luperto Sinni E (1996) Sintesi delle conoscenze biostratigrafiche del cretaceo del Gargano e delle Murge. Memorie Società Geologica Italiana 51:995–1018

Luperto Sinni E, Borgomano J (1989) Le Crétacé Supérieur des Murges sud-orientales (Italie méridionale): stratigraphie et évolution des paléoenvironnements. Riv Ital Paleontol S 95(2):95–136

Molina E, Cultrone G, Sebastian E, Alonso FL, Carrizo L, Gisbert J, Buj O (2011) The pore system of sedimentary rocks as a key factor in the durability of building materials. Eng Geol 118:110–121

Mutluturk M, Altindag R, Turk G (2004) A decay function model for the integrity loss of rock when subjected to recurrent cycles of freezing–thawing and heating–cooling. Int J Rock Mech Min 41:237–244

Ricchetti G, Ciaranfi N, Luperto Sinni E, Mongelli F, Pieri P (1988) Geodinamica ed evoluzione sedimentaria e tettonica dell'avampaese apulo. Memorie Società Geologica Italiana 41:57–82

Rothert E, Eggers T, Cassar J, Ruedrich J, Fitzner B, Siegesmund S (2007) Stone properties and weathering induced by salt crystallization of Maltese Globigerina Limestone. In: Prikryl R, Smith BJ (eds) Building stone decay: from diagnosis to conservation, vol 271. Geological Society London, Special Publications, London, pp 189–198

Ruiz-Agudo E, Mees F, Jacobs P, Rodriguez-Navarro C (2007) The role of saline solution properties on porous limestone salt weathering by magnesium and sodium sulfates. Environ Geol 52:269–281

Siegesmund S, Ullemeyer K, Weiss T, Tschegg EK (2000) Physical weathering of marbles caused by anisotropic thermal expansion. Int J Earth Sci 89:170–182

Sippel J, Siegesmund S, Weiss T, Nitsch KH, Korzen M (2007) Decay of natural stones caused by fire damage. In: Prikryl R, Smith BJ (eds) Building stone decay: from diagnosis to conservation, vol 271. Geological Society London, Special Publications, London, pp 139–151

Spalluto L, Caffau M (2010) Stratigraphy of the mid-Cretaceous shallow-water limestones of the Apulia Carbonate Platform (Murge, Apulia, southern Italy). Ital J Geosci (Boll Soc Geol Ital) 129(3):335–352

Tucci P, Morbidelli P (2004) Apulian marbles: recognition and characterisation of ancient quarries finalised to archaeometric aims. Ostuni District (South-Eastern Murge, Apulia, Italy). Period Miner 73:127–140

Tucci P, Morbidelli P, Imperatori C (2007) Study for restoration purposes about the obelisk located in 'Piazza della Libertà' at Ostuni (Brindisi, Southern Italy). Period Miner 76(1):59–73

Vázquez P, Acuña M, Benavente D, Gibeaux S, Navarro I, Gomez-Heras M (2016) Evolution of surface properties of ornamental granitoids exposed to high temperatures. Constr Build Mater 104:263–275

Yavuz H, Altindag R, Sarac S, Ugur I, Sengun N (2006) Estimating the index properties of deteriorated carbonate rocks due to freeze–thaw and thermal shock weathering. Int J Rock Mech Min 43:767–775

Yavuz H, Demirdag S, Caran S (2010) Thermal effect on the physical properties of carbonate rocks. Int J Rock Mech Min 47:94–103